Buttling, S., Fellenius, B.H., and Pinijpol, N., 2024. A case history of nine years of monitoring a wide pile group. Institution of Civil Engineers, ICE, Geotechnical Engineering, 177(2) 13 p. doi.org/10.1680/jgeen.23.00001.

Cite this article
Buttling S., Fellenius B.H,. and Pinijpol N., 2024
A nine-year case history of monitoring a wide pile group. *Proceedings of the Institution of Civil Engineers – Geotechnical Engineering*, 177(2) 13 p. https://doi.org/10.1680/jgeen.23.00001

Research Article
Paper 2300001
Received 04/01/2023;
Accepted 23/01/2024;
First published online 29/04/2024

Geotechnical Engineering

A nine-year case history of monitoring a wide pile group

1 **Stephen Buttling** BSc(Eng), ACGI, PhD, CPEng, FIEAust, NER, APEC Engineer, IntPE(Aust), RPEQ
Principal, National Geotechnical Consultants, Brisbane, Australia
(corresponding author: stephen.buttling@ngconsult.com.au)

2 **Bengt H. Fellenius** MSc, DrTech, PEng
Consulting Engineer, Sidney, Ontario, Canada

3 **Naruedol Pinijpol** BEng, MEIT
Senior Project Manager, NGC Thailand, Bangkok, Thailand



This is the first of two papers on a wide pile group. The geology and a geotechnical model of the site are presented, along with the design of a single pile, analysis of a static loading test, and some dynamic tests. Response of the piled foundations comprising 399 bored piles supporting three 70-storey towers on a common mat was monitored. Records consist of results of a static loading test, dynamic tests of four piles, the development of load in 15 piles, and settlement of 40 points during construction and nine years following. At end of construction, the perimeter piles received more load from the towers than did the interior piles and the mat settled on average 90 mm. By the end of the monitoring period, due to the general subsidence, the average settlement of the mat had increased by 50 mm. Most of the settlement is considered to originate from the compression of the soil layers below the pile toe level. A subsequent paper will present the analysis and design of the wide pile group, and the numerical analysis of the static loading test on a single pile and of the wide pile group.

Keywords: field instrumentation/foundations/monitoring/piles & piling/rafts/settlement/soil/structure interaction

Notation

a	empirical modulus modifier, depending on soil type
B	raft width
c'	apparent cohesion
E_r	Young's modulus of raft
E_s	Young's modulus of soil
K_{rs}	stiffness ratio
L	raft length
m	modulus number
m_v	coefficient of volume compressibility
q_{tM}	stress-adjusted (depth-adjusted) cone resistance (kPa)
s_u	undrained shear strength
t_r	raft thickness
ν_r	Poisson's ratio of raft
ν_s	Poisson's ratio of soil
σ_r	reference stress = 100 kPa
ϕ'	effective angle of internal friction

1. Introduction

Three 70-storey towers were constructed during 2006 to 2009 at South Sathorn Road in Bangkok, Thailand (Figure 1). The towers were situated side by side on a common mat foundation, 36×86 m in plan and 3 to 3.5 m thick. The towers were about 200 m high, each one had a central lift core, and they were braced together with storey height trusses in both horizontal directions at three levels. The mat was supported on a total of 399, 1000 mm dia., 48.5 m long bored piles, spaced equilaterally at a centre-to-centre distance (c/c) of 3.0 m. The average stress on the mat foundation was about 520 kPa.

A site investigation typical of those common in Bangkok was carried out within the site plan dimensions of about 180×200 m, with six boreholes to 80 m depth, another five boreholes to 60 m depth and, unusually, five cone penetration tests (CPTu) to refusal at depths of about 20 to 30 m with five dissipation tests. Standard laboratory tests were carried out, again as typical for a site investigation in Bangkok, proceeding through interactions with the structural engineer to determine appropriate pile sizes, layouts and loads. The adequacy of the design was then confirmed at the start of the construction by a head-down static loading test on a pile instrumented with three equilaterally placed vibrating wire (VW) strain gauges at each of ten levels. The test pile was constructed on 8 September 2005, and tested on 10–12

October 2005. After pile construction, but before casting the mat, 15 piles were instrumented with one pair of strain gauges placed below the mat level. Readings of the 15 gauges started on 3 October 2006, before casting the mat, and continued for 917 days until 7 April 2009, the end of construction. After casting the mat, 40 markers in total were installed and mat settlement was monitored from 29 January 2007, during the remaining 1000 days of construction of the towers, then continued until 28 April 2016, 8.5 years after the end of construction. This paper is an expansion of Buttling and Zhong (2017).

2. Geological setting and site investigation

Bangkok sits on the flood plain of the Chao Prayah River, which extends about 400 km in the north–south direction –

Figure 1. The completed towers

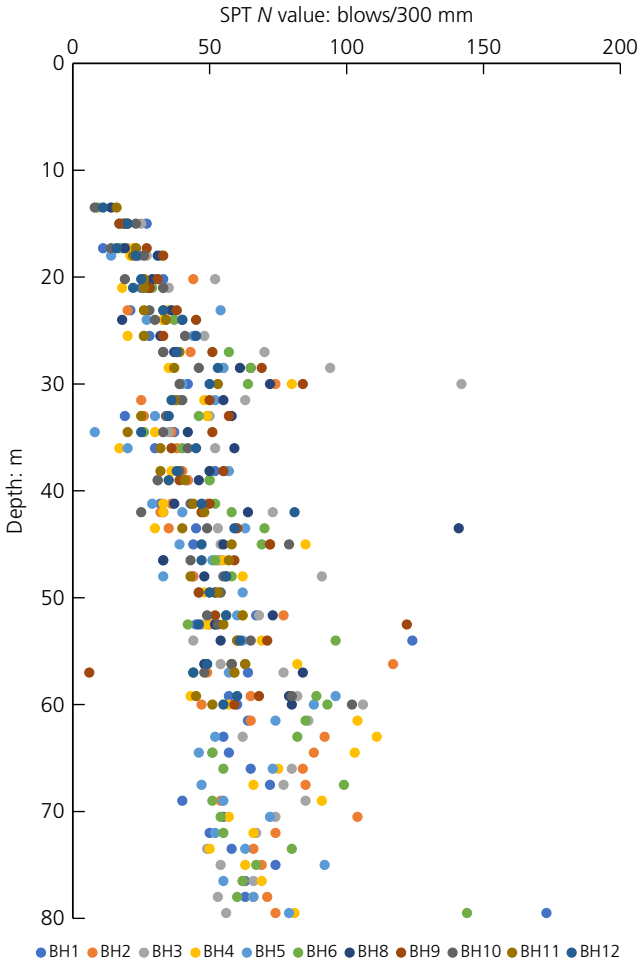

Figure 2. Profile of standard penetration test (SPT) *N* values

Table 1. Soil parameters used in design and modelling

Stratum	Typical depth to top of stratum	Weight density	Moisture content	Liquid limit	Percentage fines: %	c'	ϕ'	m_v	OCR
Made ground	G.L.								
Bangkok soft clay	1.5 to 2	14.7–17.4	48.2–83	56.7–95.1		0	20		
First stiff clay	12.5 to 16	18–20.2	21–38.6	31.3–69.3		0	25		
First sand layer	20 to 23.5				18–33		36		
Second stiff clay	35.5 to 37.5	19.3–20.6	18.5–24.6	28.9–56.1		0	26	5.9×10^{-5}	1.5
Second sand layer	38.5 to 45				10–26		38		
Third stiff clay	46 to 49.5	18.5–21.2	14.9–27.8	37.4–67	44–48	0	26		1.5
Third sand layer	57 to 65				9–22		40		
Fourth stiff clay	68.5 to 76	19.6–21	15.1–21.7	49.5–63.9	12	0	20		1.5

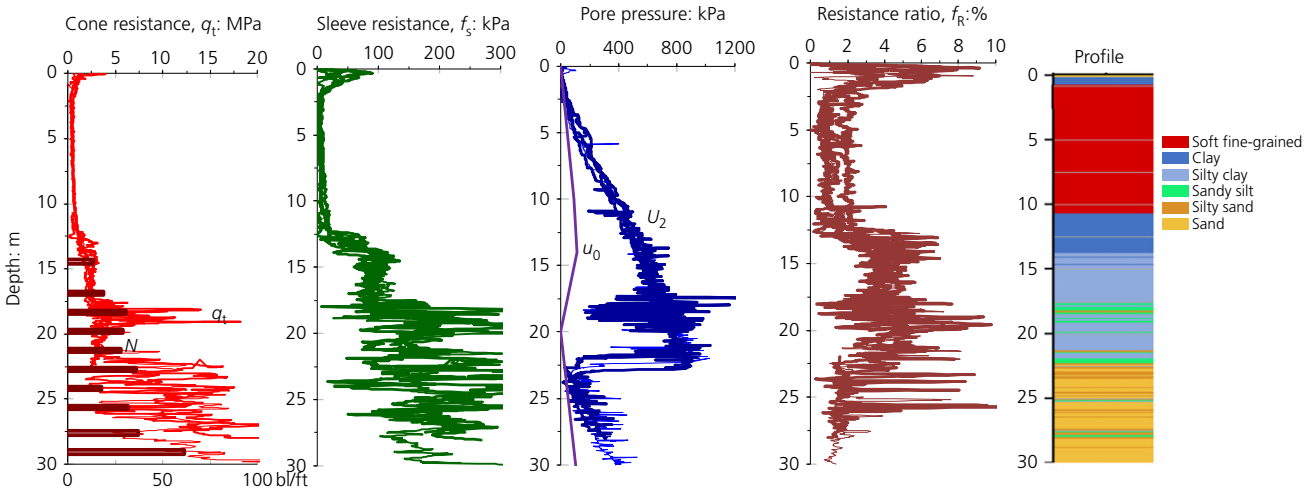

Figure 3. Soil profile from piezocone tests (CPTu) and bore holes

from the confluence of the Nan and Ping rivers to the Gulf of Thailand – and about 180 km in the east–west direction. Numerous marine transgressions have created a soil profile comprising alternating layers of sands and clays, laid down in marine, deltaic and fluvial environments above bedrock at depths of about 500 to 1000 m (Balasubramaniam *et al.*, 2004). The uppermost layer is a Holocene soft marine clay, which has a crust of desiccated clay and anthropogenic deposits.

In the site investigation split-spoon soil samples were obtained in coarse-grained soil layers, while in fine-grained soil layers, Shelby tube samples were obtained until the tubes could not be pushed deeper, which was between 10 and 20 m above the termination depth for the 80 m deep holes, and about 5 m above the termination depth for the 60 m deep holes.

The site explorations showed that the soft Bangkok Clay extends to a depth of about 13 m and is followed by underdrained first stiff clay to between 18 and 22 m above the first sand layer. This last contains a number of interbedded layers and reaches about 36 m depth, before giving way to the second stiff clay above the second sand layer to between 43 and 48 m, and then the third stiff clay reaching between 57 and 64 m.

A geotechnical model has then been produced, based on this site-specific investigation together with experience in Bangkok over a 16 year period including more than 20 instrumented static load tests, and published data. Table 1 shows the ranges of values for several key parameters. For pile design, the standard penetration test (SPT) N values were used, as illustrated in Figure 2, with a relationship between SPT N value and undrained shear strength

1. $s_u = 6.7 \times N$ kPa

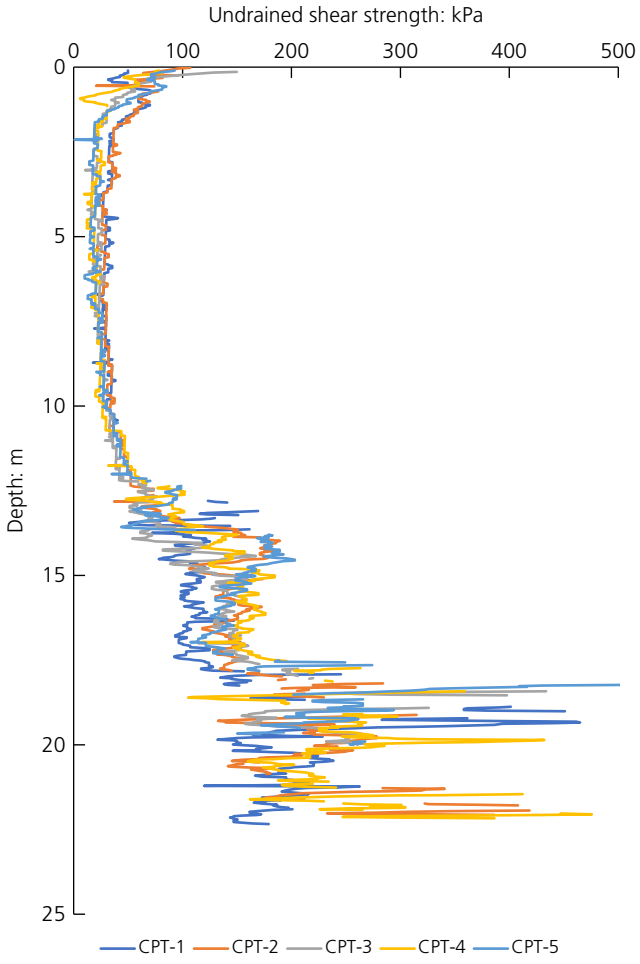

Figure 4. Undrained shear strength profile from CPTu tests

proposed by Weeranan (1983), reported by Pichit *et al.* (1987) and verified by the static tests mentioned. This is noted to be higher than the factor of 5 proposed by Stroud (1988) for

clays with a plasticity index of 15% < PI < 50%, but is counteracted by the use of an α value of 0.42, rather than the 0.5 recommended by Stroud.

Figure 3 combines the five CPTu soundings at the site, which indicate a characteristic uniformity. The CPTu q_t diagrams show that the Bangkok clay is very soft to soft to a depth of about 12 m. It is then firm to stiff or dense to the full explored depth of about 22 m. The *N*-indices of a borehole (BH-8) drilled at the test pile location are superimposed on the q_t graph, showing the soil below the Bangkok Clay to be firm to stiff between about 12 and 22 m and very dense or very stiff to hard below. The CPTu soundings were terminated at a depth of less than 25 m, while the boreholes were taken to about 80 m. The CPTu test data have been processed to provide other parameters considered to be useful in further analyses. Figure 4 shows the variation of undrained shear strength with depth derived from the CPT soundings.

Figure 5 shows the range of compressibility derived from the soundings as expressed by the distribution of Janbu modulus number (Janbu, 1963a, 1963b, 1998). The distribution was determined using the method proposed by Massarsch (1994) as the semi-empirical relationship shown in Equation 2 between the modulus number and the cone resistance adjusted for depth (Fellenius, 2024).

$$m = a\left(\frac{q_{tM}}{\sigma_r}\right)^{0.5} \quad (2)$$

where m is the modulus number; a is the empirical modulus modifier, which depends on soil type; q_{tM} is the stress-adjusted (depth-adjusted) cone resistance (kPa); and σ_r is the reference stress = 100 kPa

The distributions illustrate the consistent uniformity of compressibility with depth of the Bangkok clay. No oedometer tests were carried out on samples from the site. In the absence of actual measured compressibility that could be used for calibration of the Massarsch (1994) CPT method, the m distributions have been derived applying the same modulus modifier of 3.0 to all records, as typical of soft clays. The distribution of the overconsolidation ratio (OCR), also derived from the CPTu data, is shown in Figure 6.

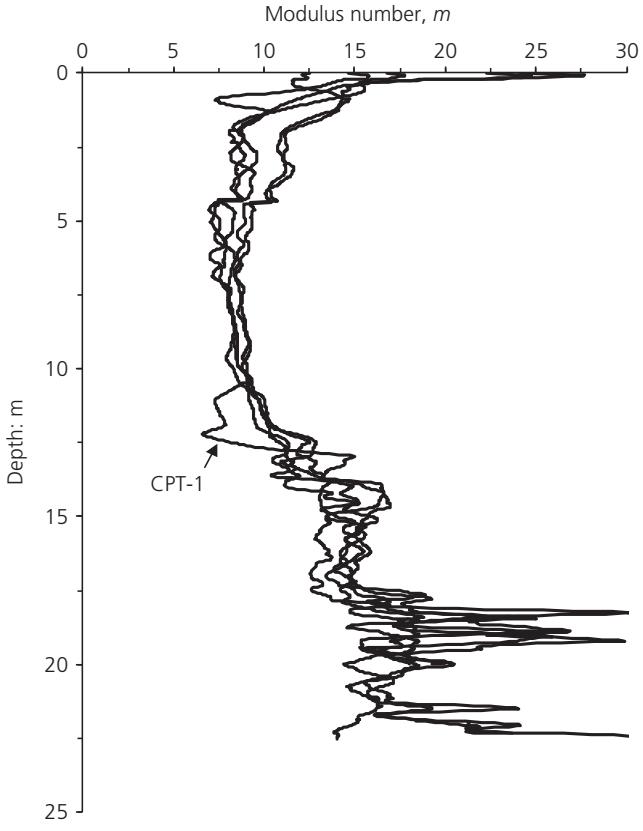

Figure 5. Profile of modulus number, *m*, derived from CPTu tests

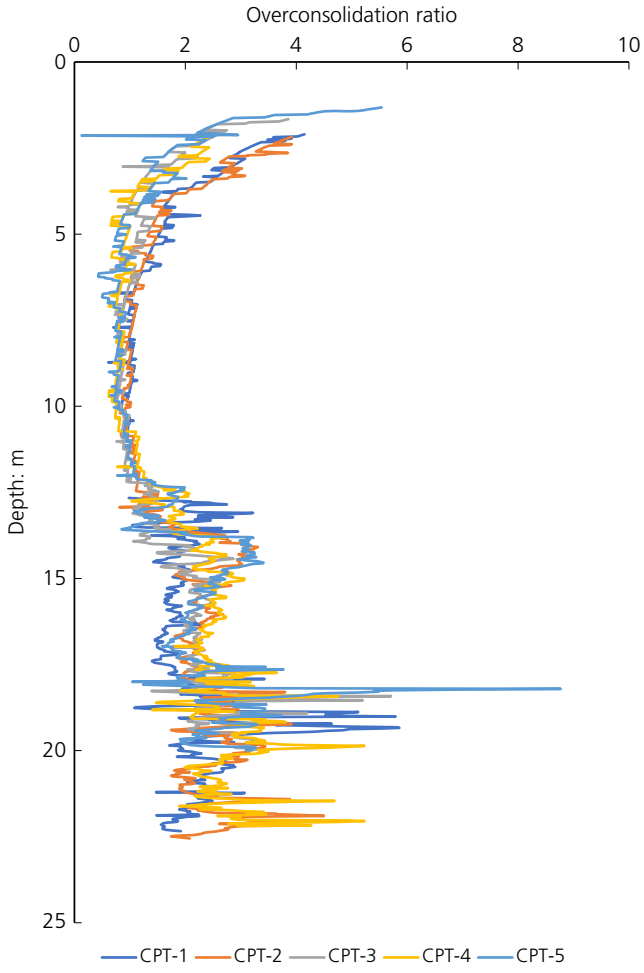

Figure 6. Overconsolidation ratio (OCR) profile inferred from CPTu tests

3. Groundwater

A perched groundwater level lies close to the ground surface, associated with surface rivers and canals (known locally as khlongs), but below this the phreatic surface drops to about 20 m below ground level, after which it again becomes hydrostatic within the range of measurements from the surface. This drawdown is because Bangkok has, for many decades, been subjected to mining of water for commercial, industrial, agricultural and domestic use from the numerous aquifers within the soil profile, especially in the upper 200 m, as seen in Figure 7, with the profile of piezometric head with depth shown in Figure 8. This shows data with hollow diamonds from the subject site, which are confirmed by the data with solid circles from a site less than 500 m away. Measurements in other aquifers at a depth of 100 to 200 m show the phreatic level drawn down to about 60 m.

The water mining has been primarily from three main aquifers:

- Phrapradaeng – 100 m depth
- Nakhonluang – 150 m depth
- Nonthaburi – 200 m depth.

The water mining has resulted in significant general subsidence, which has led to differential settlement between the ground surface and piled foundations. The mitigation measures adopted recently, comprising a pricing policy for groundwater management and strict enforcement of groundwater laws, have resulted in a reduction in groundwater mining. However, the land subsidence will continue for a long while owing to the time-dependent consolidation behaviour of the soft clay layer and clay aquicludes. At the site, the subsidence is believed to amount to about 10 mm per year over recent years.

4. Static loading test

At the start of the pile construction, a head-down static loading test was carried out on a vibrating wire (VW)-gauge instrumented test pile (Italthai Trevi, 2005). The bored pile, 48.5 m long and 1 m dia., was constructed on 8 September 2005, to a pile-head (cap) level about 0.8 m above the ground surface, and tested on 10 October 2005. The reaction load was provided by four reaction piles placed at 4.5 m c/c distance from the test pile. Ten levels of VW-gauges, SG1 through SG10, were placed in the pile at 1.5, 15.0, 19.0, 23.0, 27.0, 31.5, 35.5, 39.5, 43.5 and 47.0 m depths below the pile head. The pile cap base was about level with the ground surface. Two telltales were installed with ends at 27.0 and 47.0 m depths to measure pile compression between the pile head and the telltale end. The applied load was monitored by a separate load cell. Pile head movements were measured with reference to a beam on supports placed 3.6 m from the test pile centre and 2.55 m from the nearest anchor pile centre. The testing programme included a maximum test load of 16 800 kN,

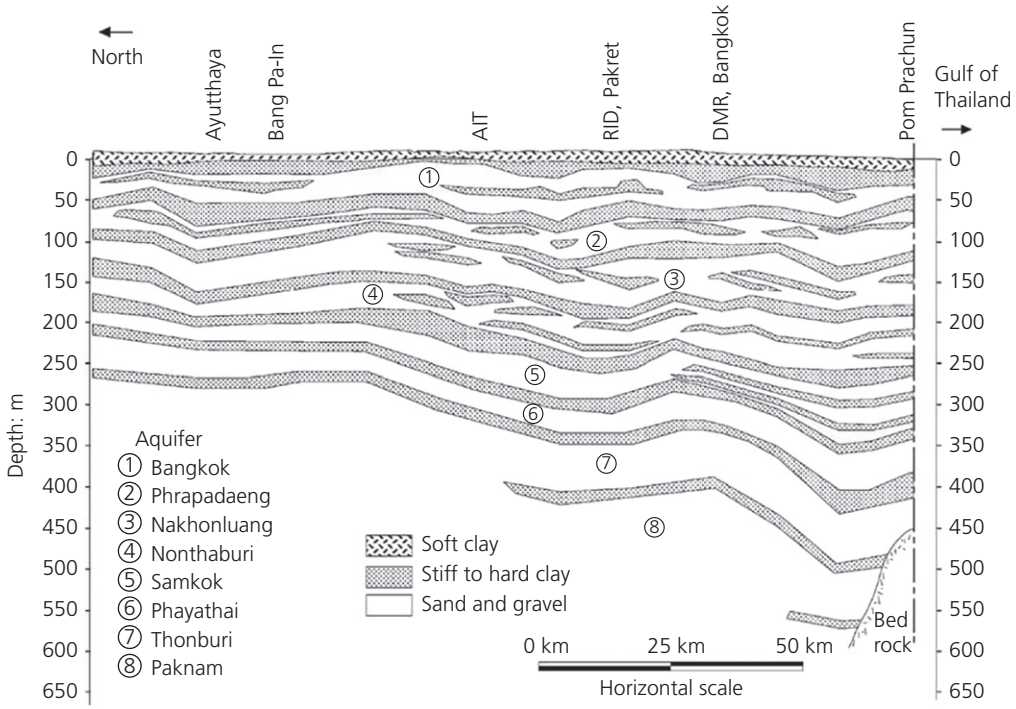

Figure 7. Hydrogeological profile through Bangkok (after Phien-wej *et al.*, 2006). AIT, Asian institute of technology; RID, royal irrigation department; DMR, department of mineral resources

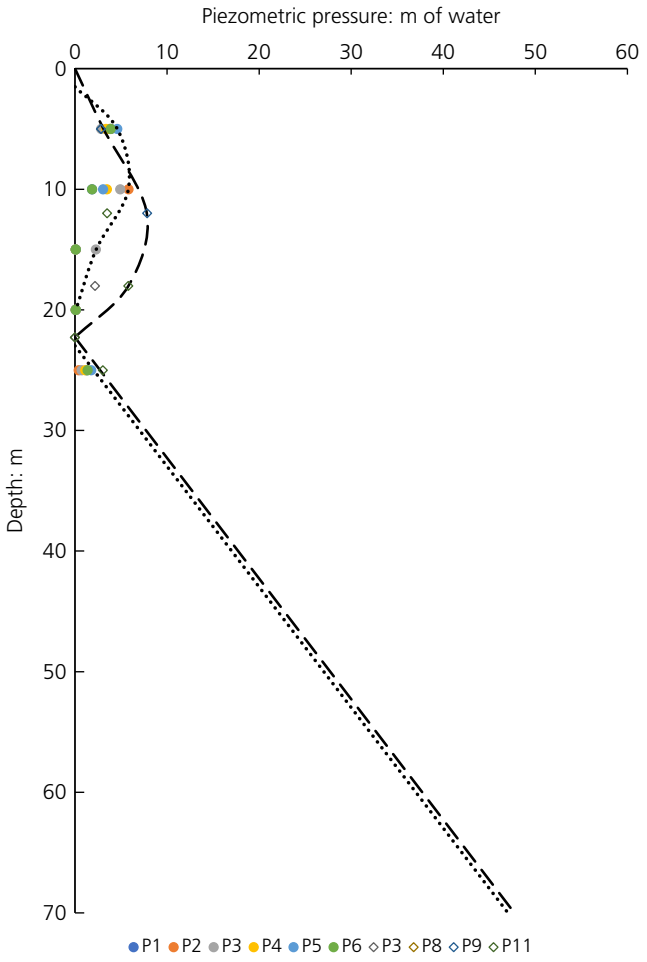

Figure 8. Shallow groundwater profile in Sathorn Road

equivalent to 100% of the design verification load plus 150% of the safe working load, in accordance with local practice. There was one unloading–reloading event up to 6475 kN and the load increments were nominally 1600 kN, applied for times until a limiting rate of movement had been reached. These varied between 30 and 60 min (stage 1) and between 90 and 150 min (stage 2). Figure 9 shows the actual applied loads plotted against time.

Figure 10 shows the applied load plotted against measured movements of the pile head and telltales. The maximum pile-head movement was small, 21 mm. The telltale movements appear to have an error of about 1 mm; this was most likely due to guide-pipe friction. The telltale to 47.0 m, 1.5 m above the pile toe, shows that the pile toe only moved about 2 mm.

The zero reference for each VW-gauge was the reading immediately before the start of stage 1. Figure 11 shows the

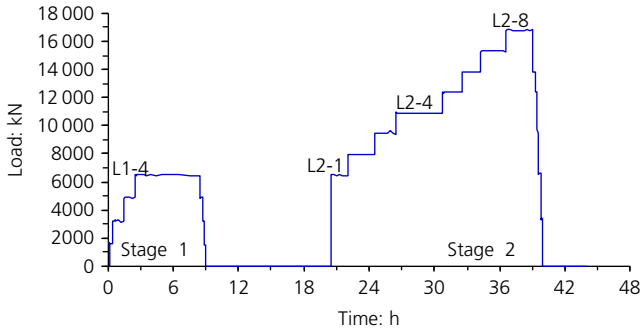

Figure 9. Applied load plotted against time

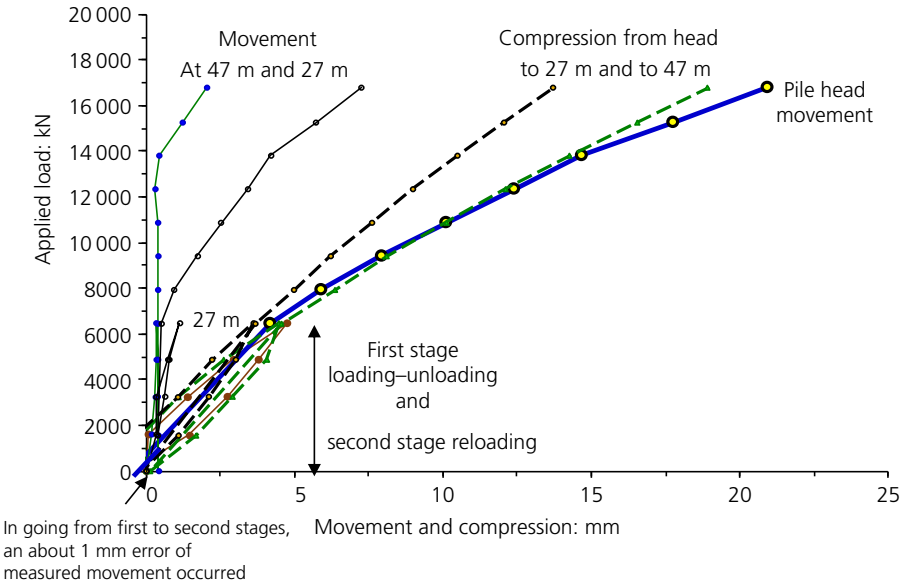

Figure 10. Applied load plotted against pile head movement and measured compression from telltales

applied load plotted against the stage 2 strains measured in the VW-gauges with stage 1 readings shown also for SG1.

The strain measurements were used to calculate the shortening between the gauge levels from the mean strain between the gauges summed up to show the compression between the pile head and the telltale ends at 27 and 47 m depths. Figure 12 shows the strain-calculated compressions together with the telltale-measured values. Both sets of curves are referenced to the pile head. The difference is significant and indicates that the telltale values are affected by friction inside the guide pipes.

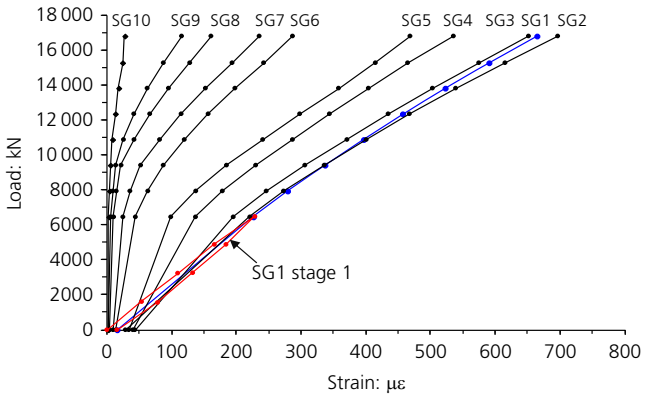

Figure 11. Applied load plotted against measured strains

As the shaft resistance between the pile head and gauge level SG1 can be assumed to be negligible, the average slope, 22.2 GN, of SG1 over the last, say, six load levels can be used to represent a likely value of axial geometric stiffness, EA, for the test pile. However, the data are sufficiently consistent for the pile geometric stiffness to be correlated to the mobilised strain, as shown in Figures 13 and 14, showing that the secant geometric stiffness, E_sA, for gauge SG1 ranged from 29.9

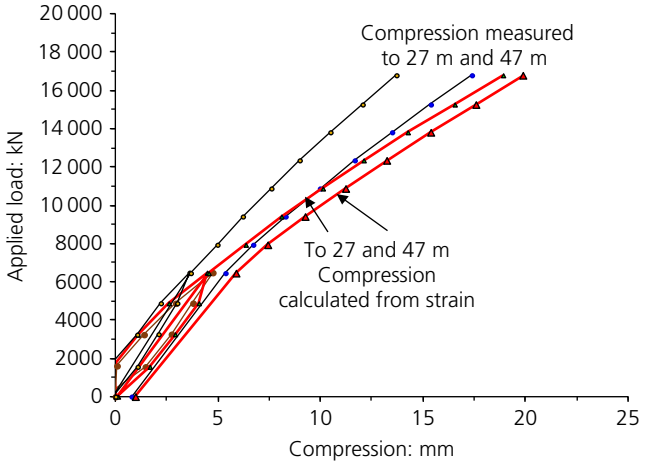

Figure 12. Applied load plotted against measured and strain-calculated compressions

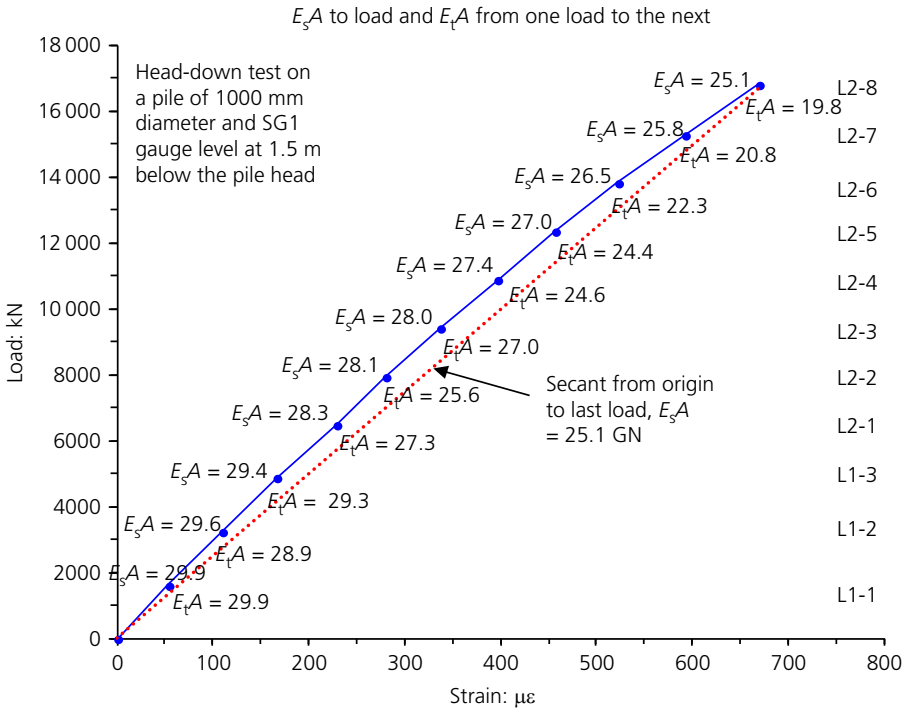

Figure 13. Applied load plotted against measured strains with incremental secant and tangent stiffness, E_sA and E_tA

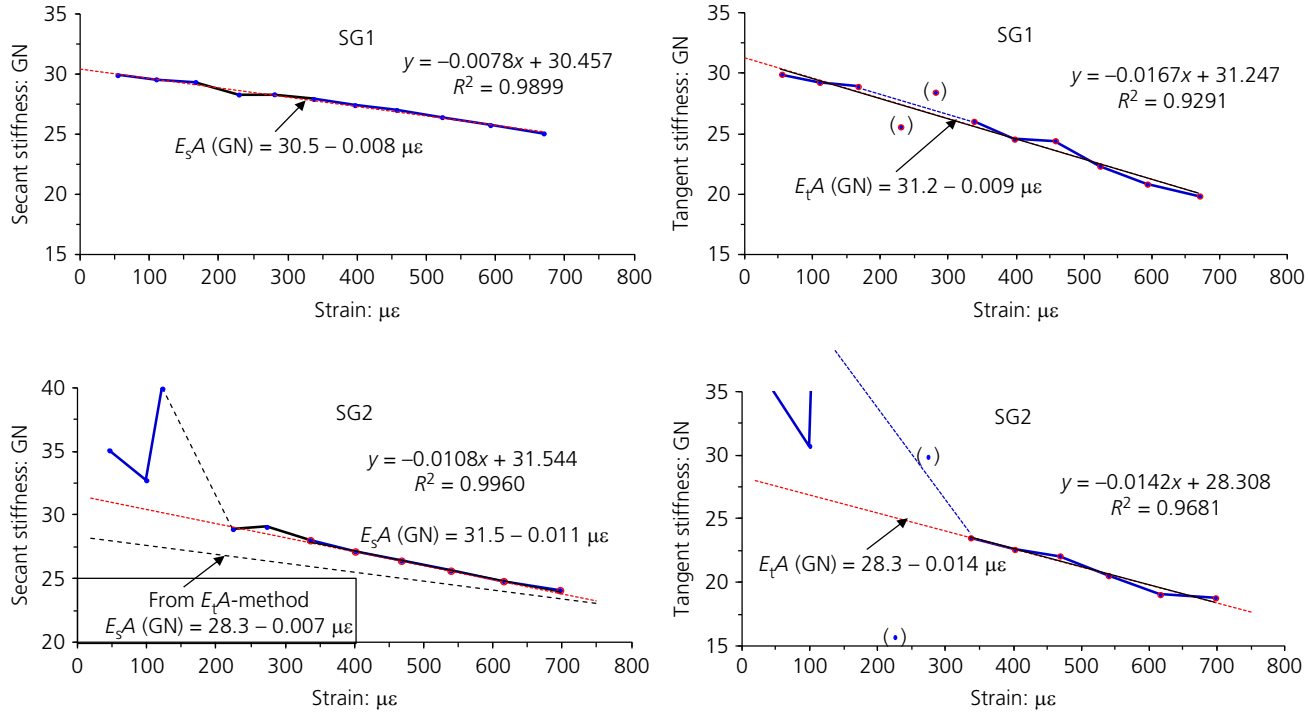

Figure 14. Secant and tangent stiffness plotted against strain for SG1 and SG2

down to 25.1 GN. Combined with the nominal pile cross-sectional area of the 1000 mm dia. pile, the E_sA value correlates to an E_s modulus ranging from 38.1 down to 32.0 GPa. Linear regression (Figure 8) of the secant geometric stiffness plotted against strain indicates a secant geometric stiffness relation of $E_sA = 30.5–0.008$ με for SG1, and this relation is the same as that determined from the tangent geometric stiffness method (Fellenius, 1989, 2023). The tangent geometric stiffness is not affected by an error in zero-reference or presence of residual force – aspects that can have a significant adverse effect on the secant geometric stiffness. The fact that the direct secant relation and the tangent relation converted to essentially equal secant relations indicates that the records for SG1 are with true zero values and that the unloading–reloading event has not adversely affected the SG1 records.

The same geometric stiffness analysis of the SG2 records does not show a similar agreement between the secant and tangent geometric stiffnesses, which indicates that the SG2 gauge was affected by an error in zero-reference or presence of residual force at the gauge level due to the unloading–reloading event. This conclusion is supported by the fact that performing the analysis after adding 30 με to each strain value brings the secant relations to agreement with the tangent relation. The E_sA-parameter adjusted in this way is about 10% smaller than that of SG1, suggesting that the pile diameter is about 4% larger at the SG2 level when compared to the diameter at the SG1 level.

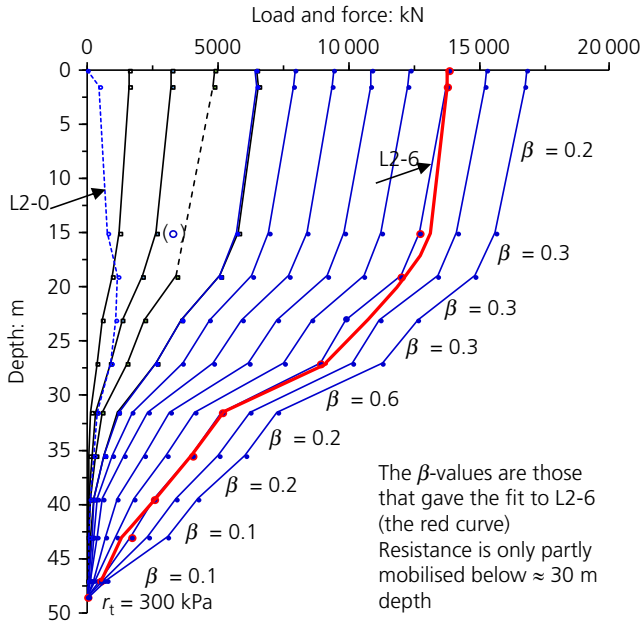

Figure 15. Load and force distributions for stage 2

Similar analyses for the gauge levels located at greater depth gave larger differences between the secant and tangent geometric stiffness relations and no assumed value of residual force could make the relations agree. That a similar stiffness analysis at

these gauge levels was unsuccessful was because the axial force had reduced with depth, the shaft resistance increased and the effect of the shear–movement (t–z) response was not plastic. Therefore, to calculate the axial force from the strain records of SG3 through SG10, the E_s–stiffness was assumed to be 90% of the relation calculated for SG1 – that is, equal to that at SG2. Figure 15 shows the force distribution determined in this way for the applied load. The red curve (at L2-6) shows a fit to the measured distribution by means of an effective stress analysis applying the listed β-coefficients for determining the shaft resistance between gauge levels. The β-coefficients are given with one-decimal precision because two-decimal precision is not warranted by the accuracy of the back-calculated force values. The slope of the force distribution curves below about 30 m depth shows that the shaft resistance was not fully mobilised and the pile toe received minimal force.

Figure 16 shows, for depth ranges of head to 15 m, 15 to 19 m, and 19 to 23 m, a plot of force between gauge level against movement. The movements are calculated from the stage 2 strain records and are referenced to zero at the start of the test – that is, no adjustment was made for the error induced by the unloading–reloading event. The curves 'Head to 15 m' and '15 to 19 m' indicate a shaft resistance more or less mobilised at very small relative movement with the subsequent response slightly strain-hardening. The very small movements between the pile and the soil show that the shaft resistance between 19 and 23 was also not fully mobilised, which made similar analysis immaterial for the resistance between gauge levels below 23 m.

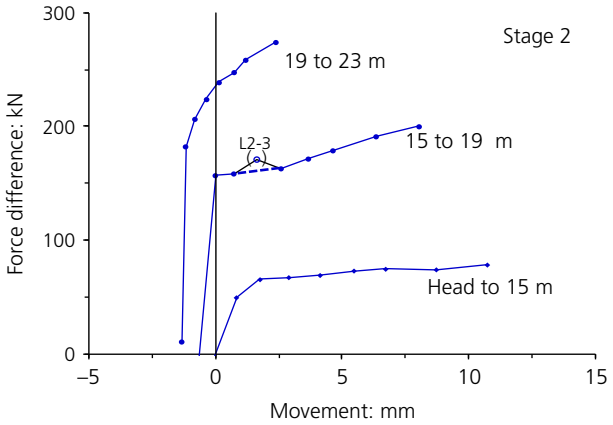

Figure 16. Stage 2 force plotted against movement between gauge levels

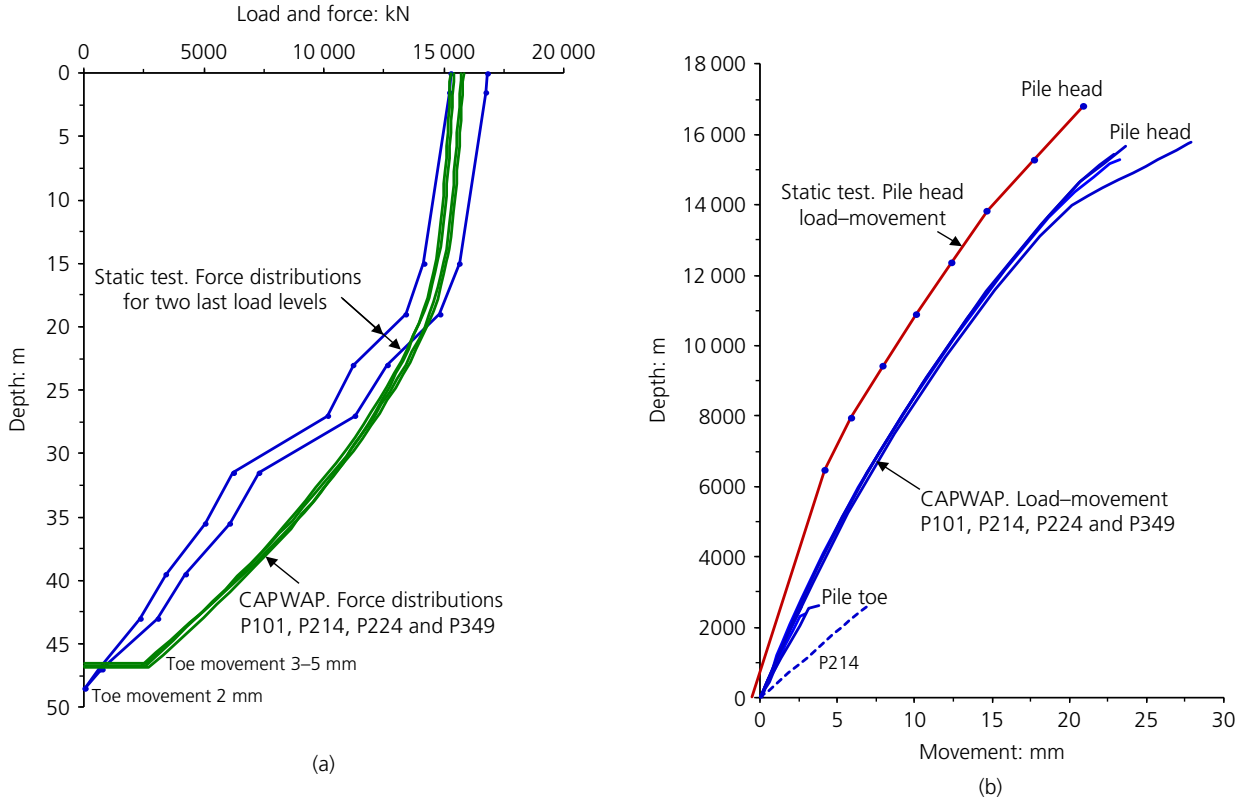

Figure 17. (a) Force distribution from CAPWAP analysis and for the two last loads in the static test; (b) Pile-head static loading tests simulated by CAPWAP and as measured in static test

Had more of the resistance been mobilised below the 23 m depth as well and, in particular, if the pile toe had been well engaged in the test – that is, the pile toe movement been larger – the data obtained then would have enabled a fit to the measured response applying t–z and q–z functions. The so-calibrated analysis could then have been employed to extrapolate the test results and allowed determination of the important response of approximately the lower third length of the pile.

5. Dynamic tests

Four of the foundation piles (P101, P214, P224, P349) were subjected to dynamic testing. The piles were constructed between 18 October and 11 December 2005, and tested on 23 January 2006, 40 to 90 days later. The dynamic tests were carried out with a 25 t drop hammer set to fall 2.00 m. The case pile wave analysis program (CAPWAP) evaluation employed an E modulus of 35 GP for all four piles. For the piles listed above, blow numbers 4, 3, 5 and 4, respectively, were used in the analyses. The measured maximum force at the pile head for the selected blows was 21.3, 24.9, 24.8 and 21.8 MN, respectively. The transferred energy for the same blows was 216, 269, 225 and 195 kJ, respectively. The report contained no information on cushions other than noting their use, and these were probably sheets of plywood.

The distribution of static force and simulated static pile-head load–movements determined in the CAPWAP analyses on the test blows are shown in Figures 17(a) and 17(b), respectively. Both the CAPWAP force distributions and the CAPWAP load–movement simulations agreed well for the four piles. The agreement was also good for the comparison to the results of the static loading test. However, because neither test had fully mobilised the pile resistance, the agreement does not lend itself to a discussion of difference in strain effect between the two test methods. The force distribution indicated a larger toe force for

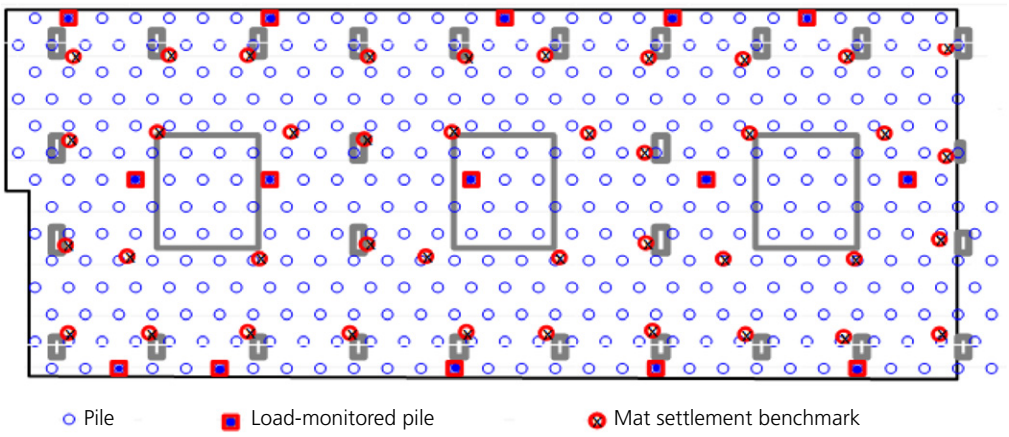

Figure 18. Layout of piles, force-monitored piles and mat-settlement points

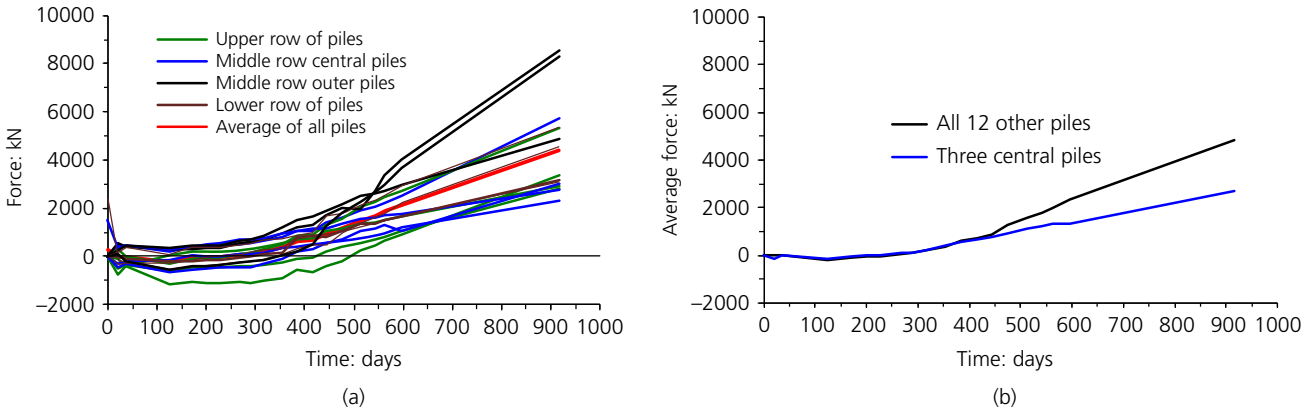

Figure 19. Force below mat plotted against time for the monitored piles: (a) considering piles in rows; (b) averages of 3 central piles and 12 outer piles

the dynamic tests, but it is not practical at this stage to ascertain whether a small adjustment to the shaft resistance between about 27.5 and 31 m depth could have improved the match quality and the agreement with the strain gauge results. It is also not possible to tell whether the dynamically tested piles had a presence of residual force as a result of downdrag. However, con-sidering the length of time before the tests, this is probable.

6. Monitoring load on 15 piles and settlement at 40 points on the mat

Figure 18 shows the layout of the piles (blue open circles) supporting the 36 × 86 m in plan and 3 to 3.5 m thick mat, so the ratio of pile spacing to mat thickness was about unity. The figure also includes the locations of the 15 piles (red squares with blue circles) that were monitored for load and the 40 settlement monitoring points. The force monitoring comprised two mat perimeter rows and one interior row of piles. The mat settlement points (red circles around X) were placed inside of the second row of piles.

The ratio of the total pile area to the total mat area, the footprint ratio (FR), is 10.1%. Horikoshi and Randolph (1997) proposed that the rigidity of a square raft can be related to its stiffness ratio, K_{rs}, expressed in Equation 3. Applying the relation to the actual rectangular raft, the stiffness ratio K_r is about 0.2. This value characterises the mat as having 'intermediate stiffness' according to relations proposed by Basile (2019); quoted by Fellenius (2024).

$$3. \qquad K_{rs} = 5.57 \frac{E_r(1-\nu_r^2)}{E_s(1-\nu_{rs}^2)} \left(\frac{B}{L}\right)^{0.5} \left(\frac{t_r}{L}\right)^3$$

where K_{rs} is the stiffness ratio; E_r is the Young's modulus of the raft; E_s is the Young's modulus of the soil; ν_r is the Poisson's ratio of the raft; ν_s is the Poisson's ratio of the soil; t_r is the raft thickness; B denotes raft width; and L is the raft length.

The forces were monitored during 917 days following completion of the pile construction until the end of the tower construction ('topping out') on 15 September 2009. Figure 19(a) shows the records of all 'VW piles' and Figure 19(b) shows the average force separated on the three central piles and the other 12 piles. The forces on the individual piles on the last day of monitoring are shown in Figure 20, in which the blue cylinders represent piles 2 to 25, the green cylinders are piles 173 to 198, and the orange cylinders are piles 374 to 389.

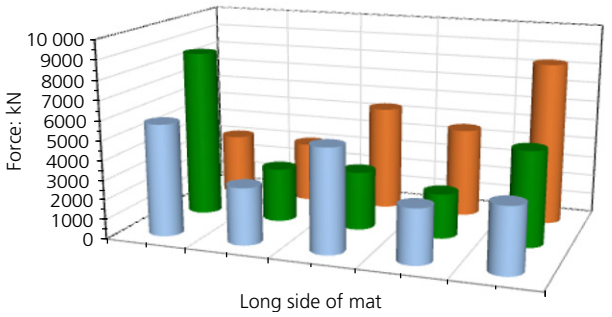

Figure 20. Three-dimensional view of the final force distribution for the piles

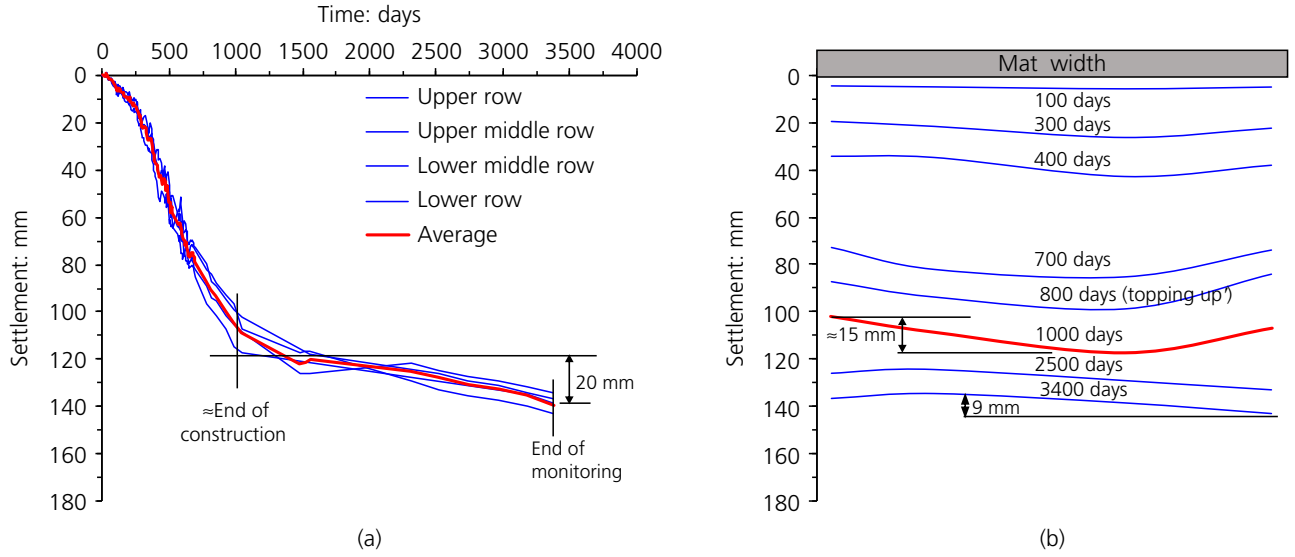

Figure 21. (a) Settlement plotted against time (days) after start of monitoring considering settlement points in rows; (b) Settlement plotted against the width of the foundation at different time intervals

Figure 21(a) shows the average settlement of the four monitored rows and Figure 21(b) shows the average settlement across the mat (from one long side to the other). During the 800 days from casting the mat, the load on the mat and piles gradually increased and the mat settled an average of 90 mm and the centre settled, on average, 15 mm more than the sides.

An average axial pile of, say, 4000 kN (as calculated from 520 kPa average mat stress over the area per pile), would cause a compression smaller than 10 mm on the 48.5 m long piles. Since the pile toe movement, although unknown, is not likely to have been more than about the same value, most of the measured 100 mm value must be caused by soil compression below the pile toe level at 48.5 m depth.

The settlement continued after the end of construction, and this is considered to be due to the soil below the pile toe level continuing to settle from the imposed tower load. The differential mat settlement reversed from the perimeter settling at the end of construction 15 mm less than the centre to settling 9 mm more on the day that monitoring was terminated. This change of the differential settlement is caused by the ongoing subsidence not so much dragging the piles down as adding force – drag force – to the perimeter piles and, thereby, increasing their compression. The settlement of the soil below the pile toe level increased, but at a diminishing rate and the total settlement was on average 140 mm when the monitoring was terminated.

7. Conclusions

The design of the foundations for the Sathorn Towers presented a challenge because of the high stress over the large mat area and the thick deposit of compressible soil coupled with the ongoing general subsidence. The head-down static loading test performed at the start of the construction was primarily intended to confirm the design, which it did with a typical degree of conservatism. With the benefit of hindsight, it did not provide the information required for an evaluation of the long-term load distribution of the foundation piles. It might have been preferable instead to perform a bidirectional test with the cell placed at about 35 to 40 m depth and designed for a maximum BD cell force of about 10 000 kN. This test would have provided more data for estimation of the long-term response of the lower length of the piles for assessing the design. However, it must be noted that, at the time, bidirectional tests had a significantly greater cost than that of the conventional head-down test used on this project and they had rarely been used on private high-rise building projects such as this.

Again, with hindsight, it is regrettable that the ground surface settlement, the site subsidence, was not monitored to serve as a reference to the mat settlement. A soil anchor or two installed to monitor the settlement below the pile toe level would have added much analytical value to the case.

The monitoring of the pile loads and mat settlement for about 9 years after the start of construction makes the project an outstanding case history of wide piled foundations. The records show that the perimeter piles received larger loads than the interior piles and that general subsidence caused the perimeter piles to settle more than the interior piles, which agrees with observations indicated by case histories on wide pile groups, especially in compressible soil, such as by Fellenius *et al.* (2019), Hansbo (1984), Hansbo and Jendeby (1998), Kakurai *et al.* (1987), Mandolini *et al.* (2005), Okabe (1977), Russo and Viggiani (1995) and Yamashita *et al.* (2013).

It should be noted that, as a case history, the authors have presented the relevant design processes without justification. Researchers who would like access to the raw data to carry out further analyses are welcome to contact the first author.

Acknowledgement

The 15 vibrating wire strain gauges installed in the bored piles were funded by a grant from the R&D Enabling Fund of the Institution of Civil Engineers (ICE), without which this work would not have been possible. The authors would like to express their gratitude to the ICE for this support.

REFERENCES

Balasubramaniam AS, Phienwej N, Gan CH and Oh YN (2004) Piled foundations and basement excavations for tall buildings in Bangkok subsoil. In *Proceedings of Malaysian Geotechnical Conference, Kuala Lumpur, Malaysia* (Sin Fatt C (ed.)). Institute of Engineers Malaysia (IEM), Kuala Lumpur, Malaysia.

Basile F (2019) The role of cap flexibility in pile group design. *Proceedings of the 17th ECSMGE, Reykjavik, Iceland*.

Buttling S and Zhong R (2017) Settlement of a high-rise building under construction – measurement and modelling. *Proceedings of the 19th ISCMGE, Seoul, Korea*. ISSMGE, London, UK, pp. 1815–1818.

Fellenius BH (1989) Tangent modulus of piles determined from strain data. In *Foundation Engineering: Current Principles and Practice* (Kulhawy FH (ed.)). American Society of Civil Engineers, New York, NY, USA, Geotechnical Special Publication 22, vol. 1, pp. 500–510.

Fellenius BH (2024) *Basics of Foundation Design – A Textbook*, electronic edition. See http://www.fellenius.net/papers/436%20The%20Red%20Book,%20Basics%20of%20Foundation%20Design%202024.pdf (accessed 22/05/2024).

Fellenius BH, Terceros MH, Terceros MA, Massarsch KR and Mandolino A (2019) Static response of a simultaneous bidirectional test on a group of 13 piles. *Proceedings of the 16th PCSMGE, Cancun, Mexico*, pp. 1214–1221.

Hansbo S (1984) Foundations on creep piles in soft clays. *First International Conference on Case Histories in Geotechnical Engineering, St. Louis, MO, USA*, pp. 259–264.

Hansbo S and Jendeby L (1998) A follow-up of two different foundation principles. *Fourth International Conference on Case Histories in Geotechnical Engineering, St. Louis, MO, USA*, pp. 259–264.

Horikoshi K and Randolph MF (1997) On the definition of raft–soil stiffness ratio for rectangular rafts. *Géotechnique* **47(5)**: 1055–1061, https://doi.org/10.1680/geot.1997.47.5.1055.

Italthai Trevi (2005) *Report on Static Pile Load Test on Instrumented Test Pile for South Sathorn Road, Bangkok*. Italthai Trevi Co. Ltd, Bangkok, Thailand.

Janbu N (1963a) Soil compressibility as determined by oedometer and triaxial tests. *ECSMFE, Wiesbaden, Germany*. ISSMGE, London, UK, vol. 1, pp. 19–25.

Janbu N (1963b) Discussion on Soil compressibility as determined by oedometer and triaxial tests. *ECSMFE, Wiesbaden, Germany*. ISSMGE, London, UK, vol 2, pp. 17–21.

Janbu N (1998) *Sediment Deformations*. Norwegian University of Science and Technology, Trondheim, Norway, Bulletin 35.

Kakurai M, Yamashita K and Tomono M (1987) Settlement behavior of piled raft foundations on soft ground. *Proceedings of the 8th ARCSMFE, Kyoto, Japan*, vol. 1, pp. 373–376.

Mandolini A, Russo G and Viggiani C (2005) Pile foundations: experimental investigations, analysis, and design. *Proceedings of 16th ICSMGE, Osaka, Japan*. ISSMGE, London, UK, pp. 177–213.

Massarsch KR (1994) Settlement analysis of compacted fill. *Proceedings of 13th ISCMGE, New Delhi, India*. ISSMGE, London, UK, vol. 1, pp. 325–328.

Okabe T (1977) Large negative friction and friction-free piles methods. *9th ICSMGE, Tokyo, Japan*. Japanese Society of Soil Mechanics and Foundation Engineering, Tokyo, Japan, vol. 1, pp. 679–682.

Phien-wej N, Giao PH and Nutalaya P (2006) Land subsidence in Bangkok, Thailand. *Engineering Geology* **82(4)**: 187–201.

Pichit J, Choochart K and Veera V (1987) Some practical interpretations of cone penetration tests for Bangkok subsoils. *Proceedings of 9th SEAGC, Bangkok, Thailand*. SEAGS, Bangkok, Thailand, vol. 1, pp. 83–92.

Russo G and Viggiani C (1995) Long-term monitoring of a piled foundation. *4th International Symposium on Field Measurements in Geomechanics, Bergamo, Italy*. ISMES, pp. 283–290.

Stroud MA (1988) The standard penetration test – its application and interpretation. *Proceedings of 1st European Symposium on Penetration Testing (ESOPT)*, vol. 2, pp. 367–375.

Weeranan P (1983) *Prediction of Pile Carrying Capacity from Standard Penetration Test in Bangkok Metropolis Subsoil*. MEng thesis, Chulalongkorn University, Bangkok, Thailand (in Thai).

Yamashita K, Wakai S and Hamada J (2013) Large-scale piled raft with grid form deep mixing walls on soft ground. *Proceedings of 18th ICSMGE, Paris, France*. ISSMGE, London, UK, vol. 3, pp. 2637–2640.